NIH Public Access
Author Manuscript
J Comput Phys. Author manuscript; available in PMC 2014 January 15.

Published in final edited form as:
J Comput Phys. 2013 January 15; 233: 315–323. doi:10.1016/j.jcp.2012.08.050.

A Low-Dispersion and Low-Dissipation Implicit Runge-Kutta Scheme

A. Najafi-Yazdi[a,*] and **L. Mongeau**[a,**]

[a]Mechanical Engineering Department, McGill University, Montreal, QC, Canada

[**]Department of Mechanical Engineering, McGill University, Macdonald Engineering Building, 817 Sherbrooke Street West, Montreal, QC, Canada H3A 2K6; Fax: +1-514-398-7365.

Abstract

A fourth-order, *implicit*, low-dispersion, and low-dissipation Runge-Kutta scheme is introduced. The scheme is optimized for minimal dissipation and dispersion errors. High order accuracy is achieved with fewer stages than standard explicit Runge-Kutta schemes. The scheme is designed to be As table for highly stiff problems. Possible applications include wall-bounded flows with solid boundaries in the computational domain, and sound generation by reacting flows.

1. Introduction

Low-dispersion and low-dissipation schemes are needed for the simulation of wave propagation phenomena such as those in computational aeroacoustics and electromagnetics. Efficient spatial discretization schemes with low dissipation and dispersion errors are available [1, 2]. But, optimal temporal integration schemes for the same purpose have received comparatively less attention. The first attempt to develop a low-dispersion and low-dissipation Runge-Kutta (LDDRK) scheme was reported by Hu *et al.* [3] who investigated single-step and two-step alternating Runge-Kutta methods. For single-step algorithms, optimal four-, five-, and six-stage explicit schemes with second-order accuracy were introduced. Fourth-order accuracy was only obtained for a six-stage scheme. Optimal 4–6 and 5–6-stage alternating schemes were also developed, which retained fourth-order accuracy. Bogey & Bailly [4] developed explicit five- and six-stage Runge-Kutta schemes. Both algorithms were of second-order accuracy. Berland *et al.* [5] extended the work of Bogey & Bailly to introduce a low-storage, fourth-order accurate optimal scheme.

The use of explicit schemes is not always desirable because of numerical stability limitations. The inclusion of solid boundaries in the flow field, or the simulation of flame/acoustic wave interactions are among the applications for which the small timestep required to maintain numerical stability may lead to prohibitive computational costs.

In the present study, a three-stage, fourth-order, *implicit*, low-dispersion, and low-dissipation Runge-Kutta (ILDDRK4) scheme is introduced. The accuracy of the new scheme is superior to the standard fourth-order explicit RK scheme for moderate- to high-

© 2012 Elsevier Inc. All rights reserved.

*Corresponding author. Address: Department of Mechanical Engineering, McGill University, Macdonald Engineering Building, 817 Sherbrooke Street West, Montreal, QC, Canada H3A 2K6; Fax: +1-514-398-7365.

Publisher's Disclaimer: This is a PDF file of an unedited manuscript that has been accepted for publication. As a service to our customers we are providing this early version of the manuscript. The manuscript will undergo copyediting, typesetting, and review of the resulting proof before it is published in its final citable form. Please note that during the production process errors may be discovered which could affect the content, and all legal disclaimers that apply to the journal pertain.

$watermark-text
$watermark-text
$watermark-text

$watermark-text

$watermark-text

$watermark-text

frequency waves, while it retains comparable accuracy for low-frequency waves. Moreover, the new scheme is designed to be A-stable to maintain numerical stability for large timesteps. The proposed scheme is significantly more accurate than the three-stage, fourth-order, singly diagonal implicit Runge-Kutta (SDIRK) scheme for almost the same computational cost.

The paper is organized as follows. A brief introduction to dispersion and dissipation errors in Runge-Kutta schemes is presented in Sec. 2. Section 3 presents the derivation of the new scheme. Some numerical examples are provided in Sec. 4. Conclusions are drawn in Sec. 5.

2. Dispersion and Dissipation Errors of Runge-Kutta Schemes

Given a differential equation of the form

$$\frac{\mathrm{d}y}{\mathrm{d}t}=f(y,t)y(0)=y0, \quad (1)$$

a P-stage Runge-Kutta can be used to approximate the function y at timestep $n+1$ from the solution at timestep n as

$$y_{n+1}=y_n+\Delta t\sum_{\alpha=1}^{P}b_\alpha F_\alpha, \quad (2)$$

where

$$F_\alpha=f(y_n+\sum_{\beta=1}^{P}\alpha_{\alpha\beta}F_\beta, t_n+c_\alpha\Delta t)\alpha=1\ldots P. \quad (3)$$

If $\alpha_{\alpha\beta}=0$ for $\beta\geq\alpha$, the scheme is explicit; otherwise it is implicit and requires an iterative procedure to obtain F_α. A convenient way to represent a Runge-Kutta scheme is the coefficient table suggested by Butcher [6],

$$\begin{array}{c|c} \mathbf{c} & \mathbf{A} \\ \hline & \mathbf{b}^T \end{array}, \quad (4)$$

where the vector **c** corresponds to the positions of stage values within the timestep. Matrix **A** is the matrix of $\alpha_{\alpha\beta}$'s in eq.(3). A lower triangular matrix **A** with null elements on the diagonal corresponds to an explicit scheme. Vector **b** corresponds to the weight coefficients, b_α, in eq.(A.2).

Consider the following linear differential equation

$$\frac{\mathrm{d}y}{\mathrm{d}t}=-i\lambda y(t). \quad (5)$$

For a P-stage Runge-Kutta method, the vector $\mathbf{Y_{n+1}}$, made up from the stage solutions for the timestep $n+1$

$watermark-text

$$Y_{n+1}^T = [y_1 y_2 \ldots y_P], \quad (6)$$

satisfies the identity

$$Y = \mathbf{1} y_n - i\Delta t \lambda \mathbf{A} \boldsymbol{Y} = \mathbf{1} y_n - i\sigma \mathbf{A} \boldsymbol{Y}, \quad (7)$$

where

$$\sigma = \lambda \Delta t. \quad (8)$$

Equation (7) can be solved for **Y** to obtain

$$\boldsymbol{Y} = (\mathbf{I} + i\sigma \mathbf{A})^{-1} \mathbf{1} y_n. \quad (9)$$

The solution at timestep $n + 1$ can then be written as

$$\begin{aligned} y_{n+1} &= y_n - i\Delta t \lambda \mathrm{b}^T \boldsymbol{Y} \\ &= y_n - i\sigma b^T (\mathbf{I} + i\sigma \mathbf{A})^{-1} \mathbf{1} y_n \quad (10) \\ &= G(z) y_n, \end{aligned}$$

where the numerical amplification factor, $G(z)$, is given by

$$G(\sigma) = 1 - i\sigma \mathrm{b}^T (\mathbf{I} + i\sigma \mathbf{A})^{-1} \mathbf{1}. \quad (11)$$

The exact amplification factor, on the other hand, is

$$G_e = e^{-i\lambda\Delta t} = e^{-i\sigma}. \quad (12)$$

An error function, $R(\sigma)$, can be defined as

$$R(\sigma) = \frac{G(\sigma)}{G_e} = |R(\sigma)| e^{i\phi}, \quad (13)$$

such that the amplification (dissipation) and phase (dispersion) errors are represented by $|R(z)|$, and the phase angle, φ, respectively. A low-dissipation and low-dispersion scheme should ensure that $|R(\sigma)| = 1$ and $\varphi = 0$ up to reasonable values of σ, which is related to the Courant-Friedrichs-Lewy (CFL) number. In fact, it can be shown that

$$\sigma = (k * \Delta x) \times \mathrm{CFL} \quad (14)$$

for a linear wave equation, where k^* is the modified wavenumber owing to the spatial discretization scheme.

3. Fourth order, implicit, low-dispersion, low-dissipation, Runge-Kutta scheme

To obtain a low-dispersion, and low dissipation Runge-Kutta scheme, the components of vectors **c, b,** and matrix **A** should be determined such that the dispersion and dissipation errors are minimized and the desired order of accuracy is maintained. In the present study, a three-stage scheme of the following form is considered:

$$\begin{array}{c|ccc} \mathbf{c_1} & a_{11} & 0 & 0 \\ \mathbf{c_2} & a_{21} & a_{22} & 0 \\ \mathbf{c_3} & a_{31} & a_{32} & a_{33} \\ \hline & b_1 & b_2 & b_3 \end{array} . \tag{15}$$

Elements α_{12}, α_{13}, and α_{23} are set to zero for the solution at one stage to be uncoupled from the solution at future stages. This facilitates the implementation, and enhances the convergence of the iterative method. Such schemes, with a lower-triangular **A**, are called *diagonally implicit Runge-Kutta* (DIRK) schemes [7]. If, in addition, all α_{ii} values are equal, the scheme is called *singly diagonally implicit Runge-Kutta* (SDIRK) [7]. The additional assumption of single diagonal elements leaves fewer coefficients that can be adjusted for optimization; therefore, the new schemes is chosen not to be SDIRK.

To retain at least fourth-order accuracy, the coefficients should satisfy the following order conditions:

$$\sum_{\alpha=1}^{3} b_\alpha = 1 \tag{16}$$

for first order accuracy,

$$\sum_{\alpha=1}^{3} b_\alpha c_a = \tfrac{1}{2} \tag{17}$$

for second order accuracy,

$$\sum_{\alpha=1}^{3} b_\alpha c_\alpha^2 = \frac{1}{3} \tag{18}$$

$$\sum_{\alpha=1}^{3}\sum_{\beta=1}^{3} b_a \alpha_{a\beta} c_\beta = \frac{1}{6} \tag{19}$$

for third order accuracy, and

$$\sum_{\alpha=1}^{3} b_\alpha c_\alpha^3 = \frac{1}{4} \tag{20}$$

$$\sum_{\alpha=1}^{3}\sum_{\beta=1}^{3} b_\alpha c_\alpha \alpha_{\alpha\beta} c_\beta = \frac{1}{8} \tag{21}$$

$watermark-text $watermark-text $watermark-text

$$\sum_{\alpha=1}^{3}\sum_{\beta=1}^{3} b_\alpha \alpha_{\alpha\beta} c_\beta^2 = \frac{1}{12} \quad (22)$$

$$\sum_{\alpha=1}^{3}\sum_{\beta=1}^{3}\sum_{\gamma=1}^{3} b_\alpha \alpha_{\alpha\beta} \alpha_{\beta\gamma} c_\gamma = \frac{1}{24} \quad (23)$$

for fourth order accuracy. The eight order condition equations, eq. (16) to (23), involve twelve unknowns for the scheme of eq.(15). Therefore, four coefficients can be adjusted to minimize the dissipation and dispersion errors. In the present study, the coefficients α_{11}, α_{21}, α_{31}, and α_{33} are chosen as the optimization parameters. As suggested by Hu *et al.* [3], the coefficients are determined to minimize the error obtained from

$$\mathrm{Err}(\Gamma) = \int_0^\Gamma \left| G(\sigma) - e^{-i\sigma} \right|^2 \mathrm{d}\sigma, \quad (24)$$

where Γ is specified according to the range of σ for which the scheme is optimized for. To ensure the stability of the scheme, the amplification error should not exceed unity for any value of σ, i.e.

$$|R(\sigma)| \leq 1 \;\; \mathrm{Re}(\sigma) \in [0, \infty). \quad (25)$$

Such schemes are called *A-stable*. Equations (24) and (25) form a constrained optimization problem which can be solved using a line search method [8]. A value of $\Gamma = 2$ is chosen for the present scheme. The parameters obtained from the optimization process are tabulated in Table A.1.

Figure A.1 and A.2 show the amplification (dissipation) and phase (dispersion) errors of the proposed scheme, along with the same information for the standard explicit fourth-order Runge-Kutta, and a-three-stage SDIRK scheme [9, 10]. Crouzeix [9] has shown that the only three-stage, A-stable, fourth order, SDIRK scheme is characterized by the following Butcher's table [10]

$$\begin{array}{c|ccc} (1+\alpha)/2 & (1+\alpha)/2 & 0 & 0 \\ 1/2 & -\alpha/2 & (1+\alpha)/2 & 0 \\ (1-\alpha)/2 & 1+\alpha & -(1+2\alpha) & (1+\alpha)/2 \\ \hline & 1/(6\alpha^2) & 1-1/(3\alpha^2) & 1/(6\alpha^2) \end{array}, \quad (26)$$

where

$$\alpha = \frac{2}{\sqrt{3}} \cos\left(\frac{\pi}{18}\right). \quad (27)$$

The proposed ILDDRK4 scheme yields significantly reduced dispersion and dissipation errors for all values of σ compared to the SDIRK scheme. The accuracy of ILDDRK4 scheme for $\sigma < 1$ is comparable to that of the standard explicit RK4 while it retains better

$watermark-text $watermark-text $watermark-text

$watermark-text

$watermark-text

$watermark-text

accuracy for $\sigma > 1$. It should also be noted that since the amplification factor is less than or equal to unity for all values of $\mathrm{Re}(\sigma) \in [0,\infty)$, the scheme is expected to be unconditionally stable. A quantitative comparison of the stability and accuracy limits of the three Runge-Kutta schemes is provided in Table A.2.

The application of the new RK scheme to nonlinear problems is straight forward. The scheme and implementation details for nonlinear conservation laws are provided in the appendix.

4. Numerical Examples

The accuracy of the scheme under investigation was compared with that of other conventional Runge-Kutta schemes for linear and nonlinear problems. A test case involving a linear wave equation is considered Sec. 4.1. Another test case involving the nonlinear Euler equations is presented in Sec. 4.2.

4.1. Linear Wave Equation

A linear wave equation of the form

$$\frac{\partial u}{\partial t}+c\frac{\partial u}{\partial x}=0 \quad (28)$$

was numerically solved using the standard fourth-order Runge-Kutta, the three-stage fourth-order SDIRK, and the proposed scheme. In all cases, a 6th-order implicit compact scheme with a seven-point stencil [1] was used for spatial discretization. An eighth-order implicit filter [11] was employed to remove high frequency saw-tooth waves. These waves have high values of wavenumbers, and grow in amplitude for the explicit Runge-Kutta. Filtering was performed at each timestep for the explicit scheme to maintain numerical stability. The filter was not needed for the implicit schemes, because the implicit schemes damp high frequency saw-tooth waves. This can be confirmed by comparing the amplification factor of the three schemes for high values of σ, as shown in Fig. A.1.

A wave speed $C = 1$ and spatial step size $\Delta x = 1$ were chosen. The initial condition was

$$u(x,t=0)=e^{-\frac{(x-x_m)^2}{b^2}} \times [\cos\ (2\pi k_1\,[x-x_m]) + \cos\ (2\pi k_2\,[x-x_m])]\,, \quad (29)$$

where $x_m = 90$, $b = 20$, $k_1\Delta x = 1/8$, and $k_2\Delta x = 1/16$. Figure A.3 show the results obtained for $t = 300$ with CFL numbers equal to 0.5 to 2. Table A.3 shows the L_2 norm of the error defined as

$$L_2(e)=\left[\int_0^{\mathrm{xmax}} (u_{ex}-u_{nu})^2 \mathrm{d}x\right]^{1/2}, \quad (30)$$

where u_{ex}, and u_{nu} represent the exact and numerical solutions, respectively. The proposed three-stage implicit scheme yields more accurate results than both the classic explicit Runge-Kutta, and the fourth-order SDIRK schemes. The explicit scheme resulted in an unstable solution at CFL number equal to 2, while the implicit schemes were stable. The discrepancy observed between the numerical results and the exact solution at such high CFL numbers is due to the dispersion error associated with a high wave number solution. The agreement between the solutions improves as the wave number of the initial signal is reduced or the grid resolution is increased.

The numerical example showed that the proposed implicit scheme is on average six times slower than the explicit scheme for the same CFL number. For the present work, no attempt

$watermark-text

$watermark-text

$watermark-text

was made to improve the computational efficiency of the scheme. The use of methods such as *Lower-Upper Symmetric Gauss-Seidel* (LU-SGS) [12, 13] will be explored in future work to improve the numerical efficiency of the new scheme.

An order of accuracy analysis was also performed to verify the nominal fourth-order accuracy of the implicit scheme. A test case with the same initial condition as eq.(29) was chosen. A mesh with a spatial step size $\Delta x = 0.5$ was chosen for the analysis. Table A.4 summarizes the numerical error of the solution at CFL values of 0.125, 0.25, 0.5, and 1. A decrease in the CFL by a factor of 2 resulted in a reduction of the error by almost a factor of 16, which is indicative of the fourth order accuracy of the proposed scheme.

4.2. Nonlinear Euler equations: One-Dimensional Case

The propagation of a one-dimensional Gaussian acoustic pulse in a mean flow was considered as a nonlinear test case. The initial perturbation had the following form

$$\left\{ \begin{array}{c} \rho = 1 + \varepsilon e^{-\frac{x^2}{b^2}}, \\ u = -1, \\ p = 1 + \varepsilon e^{-\frac{x^2}{b^2}} \end{array} \right\}, \quad (31)$$

where $\varepsilon = 0.01$, and $b = 3.0$. The domain extended from −100 to 100 with $\Delta x = 0.4$. The nonlinear Euler equations in one-dimension were considered as governing equations. Nonreflective characteristic boundary conditions [14, 15] were applied at the boundaries. The boundary conditions were implemented by modifying the flux terms to impose zero incoming waves.

The SDIRK and the new ILDDRK schemes were used for time integration. A 6th-order implicit compact scheme [1] was used for spatial discretization. The implementation of implicit Runge-Kutta time integration with the compact scheme was achieved following the work of Ekaterinaris [16]. Figure A.4 shows the density profiles obtained from both schemes for $t = 26$ at different CFL numbers. The reference solution corresponds to the numerical results obtained from standard explicit Runge-Kutta scheme at CFL=0.25. Both schemes yield results in very good agreement with the reference solution at CFL=2, as shown in Fig. 4(a). The accuracy of the solution obtained from SDIRK significantly deteriorates for larger CFL values, while ILDDRK retains reasonable accuracy. It should be noted that the pulse is not symmetric due to the presence of a mean flow. Due to the negative mean flow velocity, the peak on the left side is propagating at velocity $c + |u|$ towards the negative x-direction, while the peak on the right side is moving at velocity $c - |u|$ towards the positive x-direction. Because the propagation speed of the peak on the left side is greater, the associated dispersion and dissipation errors are more significant.

Although not shown here, simulations with CFL values of 100 and more were also performed to verify the stability of the temporal integration scheme. The simulations remained stable even for such high values of CFL, although they resulted in very poor accuracy as expected.

5. Conclusion

A three-stage, fourth-order, *implicit*, low-dispersion, and low-dissipation Runge-Kutta (ILDDRK) algorithm was developed. The accuracy of the proposed scheme is comparable or superior to that of the standard, explicit, fourth-order Runge-Kutta for moderate CFL numbers. The scheme remains stable for high CFL numbers. For almost the same

computational cost, the new scheme is significantly more accurate than the three-stage, fourth order, SDIRK scheme.

Numerical examples showed the improved accuracy of the proposed scheme as compared to the classical fourth-order Runge-Kutta, and the fourth-order, three-stage SDIRK schemes for the linear wave equation, and nonlinear Euler equations. The scheme is A-stable which makes it appealing for highly stiff problems, such as wall-bounded flows, and sound generation by reacting flows. No attempt was made to improve the computational efficiency of the new scheme. The use of methods such as *Lower-Upper Symmetric Gauss-Seidel* (LU-SGS) [12, 13] will be explored in future work to minimize the computational cost of the new scheme. The design of the low-storage format of the new scheme will also be the subject of further investigations.

Acknowledgments

The authors wish to thank Prof. David Zingg (UTIAS) for his invaluable comments and suggestions to improve this study. This work was supported in part by NIH grant R01 DC005788 (L. Mongeau, PI).

APPENDIX A

Application to Conservative Laws

In this section, the implementation of the present scheme for a system of nonlinear conservation laws in two dimensions are discussed. Implementation for higher dimensions, can follow a similar procedure.

Conisder a set of conservation equations of the following form:

$$\frac{\partial \mathbf{Q}}{\partial t}+\frac{\partial \mathbf{F}(\mathbf{Q})}{\partial \xi}+\frac{\partial \mathbf{G}(\mathbf{Q})}{\partial \eta}=0, \quad \text{(A.1)}$$

where **Q** is the vecotor of conservative flow variables, and the vectors **F**, and **G** are the flux vectors.

Assuming that the solution is known at timestep n, the flow field at timestep $n+1$ can be obtained by applying a P-stage Runge-Kutta scheme to eq. (A.1)

$$\mathbf{Q}^{n+1}=\mathbf{Q}^{n}-\Delta t\sum_{\alpha=1}^{P} b_{\alpha}\left[\frac{\partial \mathbf{F}(\mathbf{Q}_{\alpha})}{\partial \xi}+\frac{\partial \mathbf{G}(\mathbf{Q}_{\alpha})}{\partial \eta}\right], \quad \text{(A.2)}$$

where $\mathbf{Q}_{\alpha}$ is the intermediate solution at stage ? and is obtained implicitly from

$$\mathbf{Q}_{\alpha}=\mathbf{Q}^{n}-\Delta t\sum_{\beta=1}^{\alpha}\alpha_{\alpha\beta}\left[\frac{\partial \mathbf{F}(\mathbf{Q}_{\beta})}{\partial \xi}+\frac{\partial \mathbf{G}(\mathbf{Q}\beta)}{\partial \eta}\right]. \quad \text{(A.3)}$$

which can be recast as

$$\mathbf{Q}_{\alpha}+\Delta t\alpha_{\alpha\alpha}\left[\frac{\partial \mathbf{F}(\mathbf{Q}_{\alpha})}{\partial \xi}+\frac{\partial \mathbf{G}(\mathbf{Q}_{\alpha})}{\partial \eta}\right]=\mathbf{Q}^{n}-\Delta t\sum_{\beta=1}^{\alpha-1}\alpha_{\alpha\beta}\left[\frac{\partial \mathbf{F}(\mathbf{Q}_{\beta})}{\partial \xi}+\frac{\partial \mathbf{G}(\mathbf{Q}_{\beta})}{\partial \eta}\right] \quad \text{(A.4)}$$

$watermark-text $watermark-text $watermark-text

$watermark-text

$watermark-text

$watermark-text

Eq. (A.4) can be iteratively solved for $\mathbf{Q}_\alpha$ using Newton's method [17] as follows. Starting from the approximation of $\mathbf{Q}_\alpha$ at the k-th iteration a new approximation, at $k+1$-th iteration can be obtained from

$$\mathbf{Q}_\alpha^{k+1}=\mathbf{Q}_\alpha^k+\Delta\mathbf{Q}_\alpha, \quad \text{(A.5)}$$

where the vector $\Delta\mathbf{Q}_\alpha$ is the solution of

$$\left[\mathbf{I}+\Delta t\alpha_{\alpha\alpha}\frac{\partial\mathbf{A}\left(\mathbf{Q}_\alpha^k\right)}{\partial\xi}+\Delta t\alpha_{\alpha\alpha}\frac{\partial\mathbf{B}\left(\mathbf{Q}_\alpha^k\right)}{\partial\eta}\right]\Delta\mathbf{Q}_\alpha=\mathbf{R}_\alpha^k. \quad \text{(A.6)}$$

Here $\mathbf{A}$ and $\mathbf{B}$ are the flux Jackobian matrices,

$$\mathbf{A}=\frac{\partial\mathbf{F}}{\partial\mathbf{Q}}, \quad \text{(A.7)}$$

$$\mathbf{B}=\frac{\partial\mathbf{G}}{\partial\mathbf{Q}}, \quad \text{(A.8)(A.9)}$$

and $\mathbf{R}_\alpha^k$ is the residual vector given by

$$\mathbf{R}_\alpha^k=\mathbf{Q}^n-\mathbf{Q}_\alpha^k-\Delta t\alpha_{\alpha\alpha}\left[\frac{\partial\mathbf{F}\left(\mathbf{Q}_\alpha^k\right)}{\partial\xi}+\frac{\partial\mathbf{G}\left(\mathbf{Q}_\alpha^k\right)}{\partial\eta}\right]-\Delta t\sum_{\beta=1}^{\alpha-1}\alpha_{\alpha\beta}\left[\frac{\partial\mathbf{F}\left(\mathbf{Q}_\beta\right)}{\partial\xi}+\frac{\partial\mathbf{G}\left(\mathbf{Q}_\beta\right)}{\partial\eta}\right]. \quad \text{(A.10)}$$

The iterative procedure is continued untill convergence. Then, the next stage of the Runge-Kutta scheme is solved. Once the intermediate solutions at all three stages are known[1], eq. (A.2) is used to march the solution to the next timestep.

Implicite factorization can be used to faciliate the implementation and reduce the computational cost. In this approach the left hand side of eq. (A.6) is approximated with

$$\begin{aligned}\left[\mathbf{I}+\Delta t\alpha_{\alpha\alpha}\frac{\partial\mathbf{A}\left(\mathbf{Q}_\alpha^k\right)}{\partial\xi}+\Delta t\alpha_{\alpha\alpha}\frac{\partial\mathbf{B}\left(\mathbf{Q}_\alpha^k\right)}{\partial\eta}\right]\Delta\mathbf{Q}_\alpha &\approx \\ \left[\mathbf{I}+\Delta t\alpha_{\alpha\alpha}\frac{\partial\mathbf{A}\left(\mathbf{Q}_\alpha^k\right)}{\partial\xi}\right]\left[\mathbf{I}+\Delta t\alpha_{\alpha\alpha}\frac{\partial\mathbf{B}\left(\mathbf{Q}_\alpha^k\right)}{\partial\eta}\right]\Delta\mathbf{Q}_\alpha.\end{aligned} \quad \text{(A.11)}$$

Using eq. (A.11) to replace the LHS of eq. (A.6) yields

$$\left[\mathbf{I}+\Delta t\alpha_{\alpha\alpha}\frac{\partial\mathbf{A}\left(\mathbf{Q}_\alpha^k\right)}{\xi}\right]\Delta\mathbf{Q}_\alpha^*=\mathbf{R}_\alpha^k, \quad \text{(A.12)}$$

[1]As a matter of fact, there is no need to save the intermediate solutions, $\mathbf{Q}_\alpha$'s. Rather, it is recommanded to save $\frac{\partial\mathbf{F}(\mathbf{Q}_\alpha)}{\partial\xi}$ and $\frac{\partial\mathbf{G}(\mathbf{Q}_\alpha)}{\partial\xi}$ as they are already calculated at each stage to obtain the residual vector.

where

$$\left[\mathbf{I}+\Delta t\alpha_{\alpha\alpha}\frac{\partial\mathbf{B}\left(Q_{\eta}^{k}\right)}{\eta}\right]\mathbf{\Delta Q}_{\alpha}=\mathbf{\Delta Q}_{\alpha}^{*}. \quad \text{(A.13)}$$

The solution involves a two step process of solving eq. (A.12) first and then solving eq. (A. 13). It should be noted that factorization of eq. (A.11) acts as a preconditining of the linear system. Although it introduces an error of $O(\Delta t^2)$ on the LHS, the scheme remains forth order accurate as long as the residual, the righ hand side, is brought to zero through subiterations.

References

1. Lele S. Compact finite difference schemes with spectral-like resolution. Journal of Computational Physics. 1992; 103:16–42.
2. Tam CKW, Webb J. Dispersion-relation-preserving finite difference schemes for computational acoustics. Journal of Computational Physics. 1993; 107:262–281.
3. Hu F, Hussaini M, Manthey J. Low-dissipation and low-dispersion runge-kutta schemes for computational acoustics. Journal of Computational Physics. 1996; 124:177–191.
4. Bogey C, Bailly C. A family of low dispersive and low dissipative explicit schemes for flow and noise computations. Journal of Computational Physics. 2004; 194:194–214.
5. Berland J, Bogey C, Bailly C. Low-dissipation and low-dispersion fourth-order runge﹐kutta algorithm. Computers & Fluids. 2006; 35:1459–1463.
6. Butcher, J. Numerical Methods for Ordinary Differential Equations. Second Edition.. John Wiley & Sons Ltd.; 2008.
7. Hairer, E.; Wanner, G. Solving ordinary differential equations II: Stiff and differential-algebraic problems. Springer; 2010.
8. Nocedal, J.; Wright, S. Numerical optimization. Springer Verlag; 1999.
9. Crouzeix, M. Ph.D. thesis. Paris: Universite Paris VI; 1975. Sur l'approximation des equations differentielles operationelles lineaires par des methodes de Runge Kutta.
10. Alexander R. Diagonally implicit Runge-Kutta methods for stiff ODE's. SIAM Journal on Numerical Analysis. 1977; 14:1006–1021.
11. Gaitonde D, Visbal M. Pad´e-type higher-order boundary filters for the navier-stokes equations. AIAA journal. 2000; 38:2103–2112.
12. Jameson A, Turkel E. Implicit schemes and lu decompositions. Mathematics of Computation. 1981; 37:385–397.
13. Yoon S, Jameson A. Lower-upper symmetric-gauss-seidel method for the euler and navier-stokes equations. AIAA journal. 1988; 26:1025–1026.
14. Thompson K. Time dependent boundary conditions for hyperbolic systems. Journal of Computational Physics. 1987; 68:1–24.
15. Poinsot TJ, Lele SK. Boundary conditions for direct simulations of compressible viscous flows. Journal of Computational Physics. 1992; 101:104–129.
16. Ekaterinaris J. Implicit, high-resolution, compact schemes for gas dynamics and aeroacoustics. Journal of Computational Physics. 1999; 156:272–299.
17. Burden, RL.; Faires, JD. Numerical Analysis. 8th edition. Thomson, Brooks/Cole; 2006.

$watermark-text $watermark-text $watermark-text

$watermark-text

$watermark-text

$watermark-text

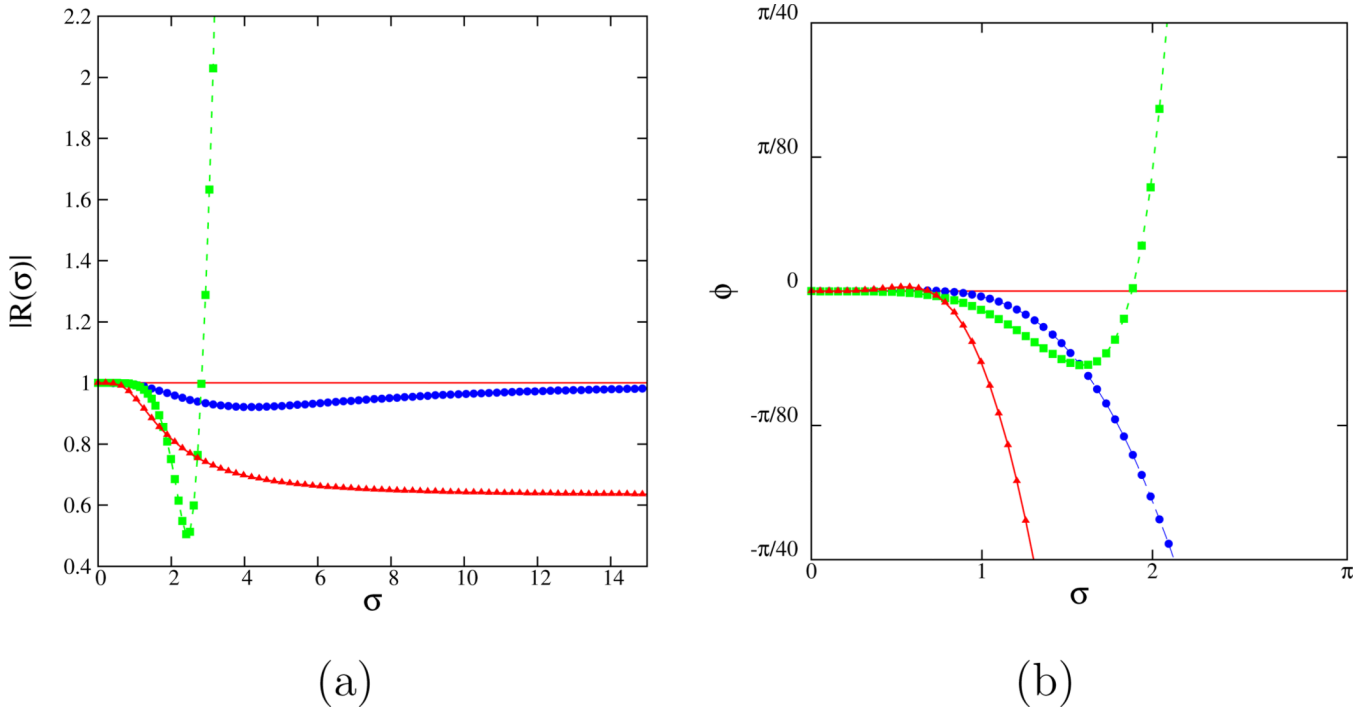

Figure A.1.

Amplification factor (a) and difference in phase of the Runge-Kutta schemes; •: the new scheme, ■, standard explicit RK4; ▲, SDIRK4.

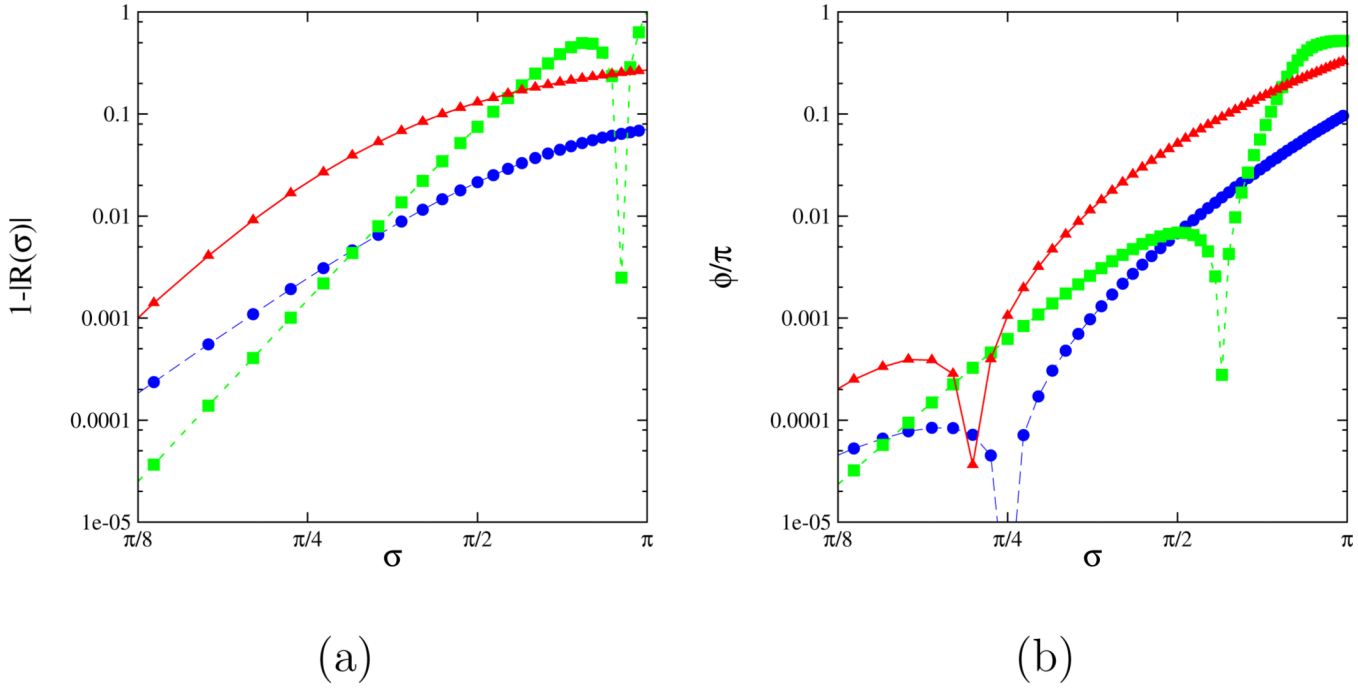

Figure A.2.

(a) Dissipation and (b) dispersion error of the Runge-Kutta schemes in logarithmic scales; •: the new scheme, ■, standard explicit RK4; ▲, SDIRK4

$watermark-text
$watermark-text
$watermark-text

$watermark-text
$watermark-text
$watermark-text

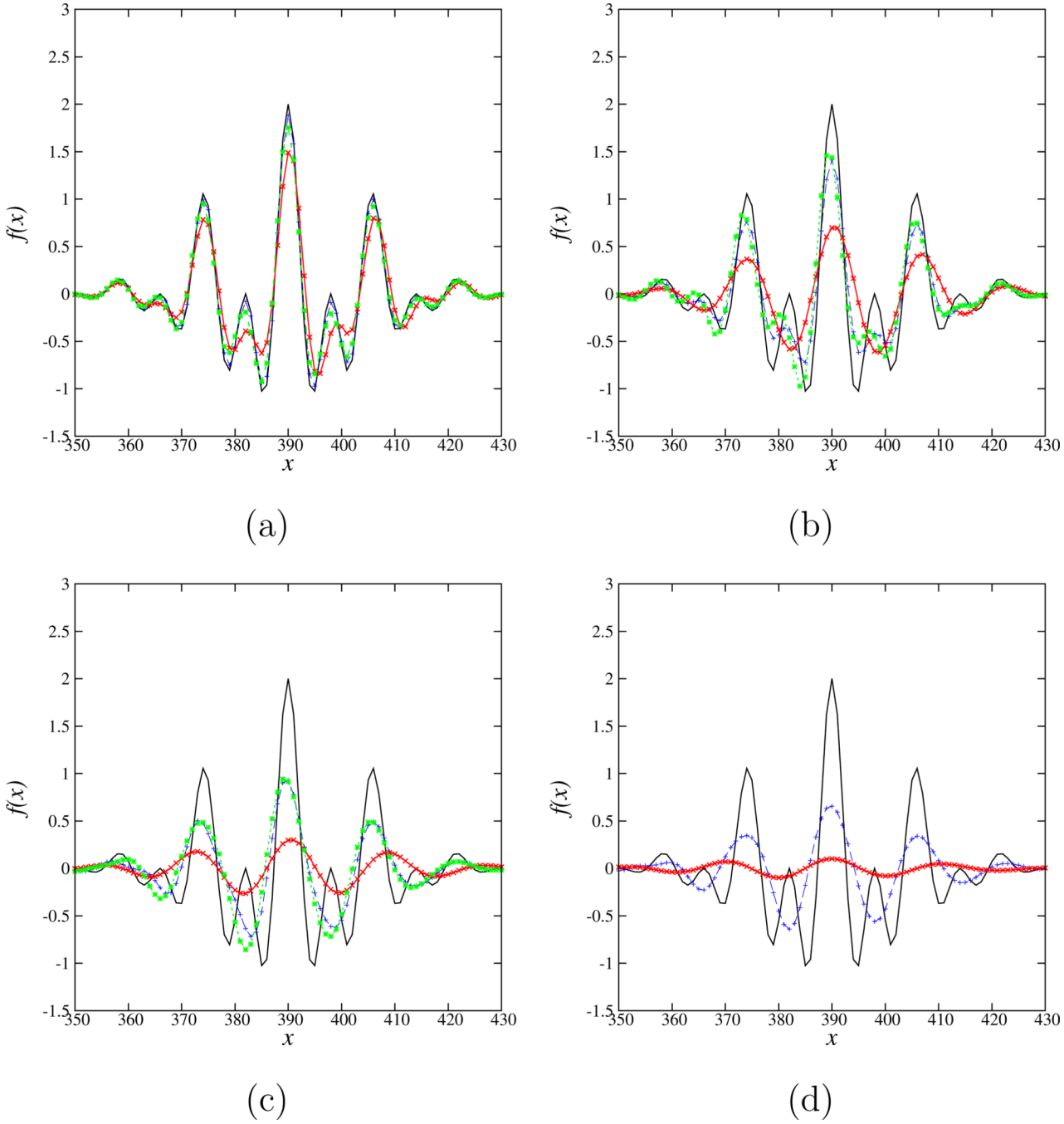

Figure A.3.
Numerical solution of eq. (28) at $t = 300$; (a) CFL=0.5; (b) CFL=1.0; (c) CFL=1.5; (d) CFL=2.0; *: standard RK4; ×: SDIRK4; +: the new scheme.

$watermark-text
$watermark-text
$watermark-text

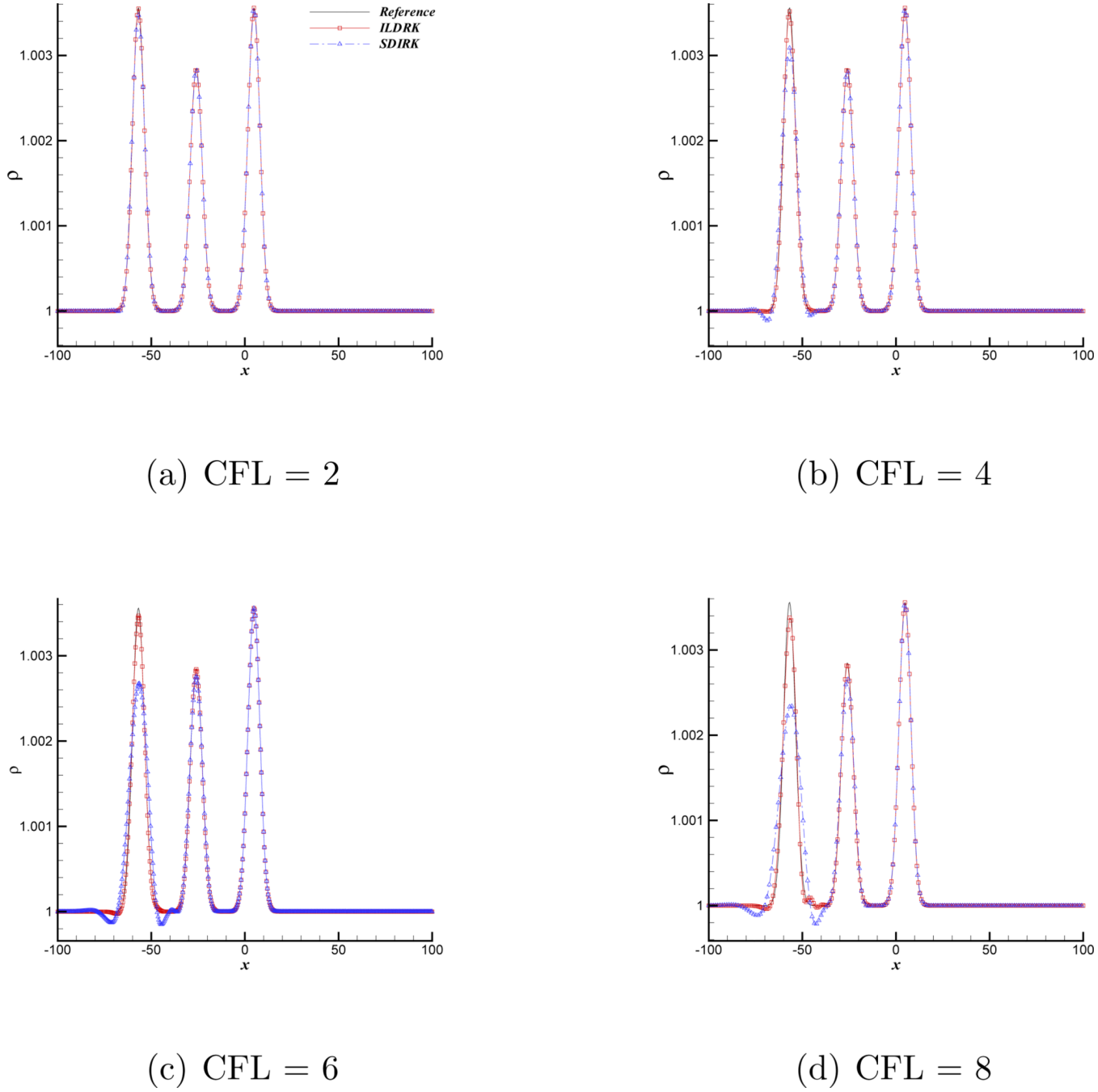

Figure A.4.
One-dimensional Gaussian pulse propagation in a uniform mean flow from left to right; The results at $t = 26.0$ are shown.

$watermark-text

$watermark-text

$watermark-text

Table A.1

Optimal coefficients for the fourth-order, implicit, low-dispersion, low-dissipation, Rung-Kutta (ILDDRK4) scheme.

Parameter	Value
a_{11}	0.377847764031163
a_{21}	0.385232756462588
a_{22}	0.461548399939329
a_{31}	0.675724855841358
a_{32}	−0.061710969841169
a_{33}	0.241480233100410
b_1	0.750869573741408
b_2	−0.362218781852651
b_3	0.611349208111243
c_1	0.257820901066211
c_2	0.434296446908075
c_3	0.758519768667167

$watermark-text

$watermark-text

$watermark-text

Table A.2

The limits of stability and accuracy for different RK schemes in terms of σ. The values correspond to $|R(\sigma)| \leq 1$ for stability, $1 - |R(\sigma)| \leq 0.01$ for the dissipation error, and $|\phi(\sigma)| \leq 5 \times 10^{-5}$ for the dispersion error.

Scheme	Stability limit	Dissipation	Dispersion
Explicit RK-4	2.828375929	1.089803638397488	0.107648123764534
SDIRK-4	∞	0.642170780547322	0.206589733458756
Present scheme	∞	1.198465101984806	0.257908675254853

$watermark-text

$watermark-text

$watermark-text

Table A.3

The L_2 norm of the error between the numerical results and the exact solution at $t = 300$.

CFL	Explicit RK-4	Present scheme	SDIRK-4
0.5	0.903517	0.581021	1.89694
1.0	2.28606	1.60723	3.74675
1.5	3.84962	1.98162	4.4246
2.0	—	3.67395	4.84705

$watermark-text

$watermark-text

$watermark-text

Table A.4

Error between the numerical results and the exact solution at $t = 300$ for different CFL numbers.

CFL	$L_2(e)$
0.125	1.17384E-5
0.25	2.00805E-4
0.5	3.21381E-3
1	4.79683E-2